

# 3D Hybrid Finite-Difference Method for Lossy Structures Based on Quasi-Static Field Solutions

Marco Kunze, *Student Member, IEEE*, and Wolfgang Heinrich, *Senior Member, IEEE*

Ferdinand-Braun-Institut (FBH), D-12489 Berlin / Germany

**Abstract** — A new 3D hybrid finite-difference (FD) method is presented that accounts for finite conductivity. The field gradients inside conductors and structural details are treated combining quasi-static field solutions with the full-wave analysis. In the quasi-static regime, the magnetic field computations and the corresponding source formulation needs special consideration. The hybrid method reduces computational efforts while maintaining accuracy of the conventional FD scheme. The new approach is verified for a MMIC coplanar short stub and airbridges.

## I. INTRODUCTION

The finite-difference method (FDM) is one of the most powerful electromagnetic simulation tools today. Nevertheless, its efficiency is still too low to meet the designers demands in terms of geometrical complexity and accuracy. This is especially true when analyzing coplanar monolithic microwave integrated circuits (MMICs), where metalization thickness and finite conductivity have to be considered [1].

In the past, enhanced FDTD methods were proposed incorporating the asymptotic field behavior around microstrip discontinuities [2],[3]. Recently, hybrid finite-difference methods for transmission-line problems were presented [4]-[6]. They are based on the finite integration scheme [7]. Line and surface integrals are multiplied with so-called correction factors. A pure numerical approach [4], based on the quasi-static approximation, and a semi-analytical method [5],[6], which uses closed-form expressions for the correction factors, are described in the literature. It has been demonstrated that the numerical efficiency can be increased significantly while achieving the same order of accuracy as with the conventional finite-difference formulation. This is due to the reduction in mesh-size. Field details like singularities and skin-effect current distribution do not need an electro-dynamic analysis. Hence, they are described by quasi-static field computations on a fine grid (i.e., with high resolution, and expressed as correction factors). The dynamic part of the analysis can then be performed on a much coarser grid.

Till today, however, a hybrid FD method for 3D problems has been proposed only for lossless structures (i.e., perfect conductors) [8]. In this contribution, a new

3D hybrid method is presented, which includes finite conductivity.

The quasi-static analysis separates in two parts. The magneto-quasi-static one is related to the currents in the conductors and thus frequency dependent. The second part is the electro-static one, which is governed by the surface charges on metalizations and frequency independent. Both quasi-static problems are solved by means of a FD approach here.

In the following, the 3D hybrid FD method is described in detail, with emphasis on the magneto-quasi-static part, which is more involved than the electro-static one. Theory is based on Maxwell grid equations, which allows for a very compact formulation. Verification is done by comparison to the conventional FD scheme [1].

## II. HYBRID FINITE-DIFFERENCE METHOD

### A. Maxwell grid equations

Our FD formulation is based on the finite integration approach [7]. This provides a one-to-one translation of Maxwell's equations on a staggered grid  $G-\tilde{G}$ . Thus, the Maxwell grid equations (MGE) for time harmonic fields in inhomogeneous, biaxial media can be written as follows:

$$\tilde{C}\vec{h} = j\omega\vec{d} + \vec{i} \quad (1)$$

$$C\vec{e} = -j\omega\vec{b} \quad (2)$$

$$\tilde{S}\vec{d} = 0 \quad (3)$$

$$S\vec{b} = 0 \quad (4)$$

$$\vec{h} = D_{\mu}^{-1}\vec{b} \quad (5)$$

$$\vec{d} = D_{\epsilon}\vec{e} \quad (6)$$

$$\vec{i} = D_{\sigma}\vec{e} \quad (7)$$

In the general form of MGEs (1)...(7) integral quantities as electric voltages  $e$ , electric currents  $i$ , electric flux densities  $d$ , magnetic voltages  $h$ , and magnetic flux densities  $b$  are collected in vectors, which contain the discretized values at the grid points.  $C, \tilde{C}, S,$  and  $\tilde{S}$  are discrete  $\nabla \times \cdot, \nabla \cdot \cdot$  operators in the staggered grid  $G - \tilde{G}$ .  $D_\mu^{-1}, D_\epsilon,$  and  $D_\sigma$  denote diagonal matrices. They are discrete representations of the material tensors  $[\mu]^{-1}, [\epsilon]$  and  $[\sigma]$ . Their elements are defined as  $h/b, d/e,$  and  $i/e$ .

The MGEs (1)...(4) are exact representations of Maxwell's equations in integral form and do not introduce discretization errors. The actual discretization occurs only when the material equations are replaced by the matrix relations (5)...(7). The MGEs (1)...(7) represent a fully general discrete replacement of the analytical Maxwell equations.

### B. Magneto-quasi-static field solution

For the quasi-static case, i.e., as far as the characteristic dimensions remain small compared to wavelength, displacement currents can be neglected. Eqn. (1) then reads

$$\tilde{C}\tilde{h} = \tilde{i}. \quad (8)$$

Combining (2), (5), (6), (7), and (8) a discrete formulation of the analytical differential equation  $\nabla \times [\mu]^{-1} \cdot (\nabla \times \tilde{E}) + j\omega[\sigma]\tilde{E} = -j\omega[\sigma]\tilde{E}_0$  can be derived. The right-hand side represents a source term. The corresponding FD equation reads

$$\left( \tilde{C}D_\mu^{-1}C + j\omega D_\sigma \right) \tilde{E} = -j\omega D_\sigma \tilde{E}_0. \quad (9)$$

An important question is the choice of the source term  $\tilde{E}_0$ . It must be divergence-free and fulfill the boundary conditions on conductor surfaces (i.e., its normal component must vanish there). In the 3D case, such a source term is not easy to find. We use the static current distribution within the metalizations of the structure under investigation. The static current distribution and the corresponding electric field can be derived from a potential. Hence, the electric voltages  $\tilde{E}_0$  are given as

$$\tilde{E}_0 = -\tilde{S}^T \tilde{\varphi}, \quad (10)$$

where  $\tilde{\varphi}$  is the vector containing the potential on any grid node (for  $\tilde{S}$ , see eqns. (3)). Equation (10) is a discrete representation of the analytical differential equation  $\tilde{E} = \nabla \cdot \phi$ . Note that this potential is defined only within the conductors. Its distribution can be found solving

$$-\tilde{S}D_\sigma \tilde{S}^T \tilde{\varphi} = 0 \quad (11)$$

which is equivalent to the differential equation  $\nabla \cdot [\sigma] \cdot \nabla \cdot \phi = 0$ . The normal component of  $\tilde{E}_0$  must vanish on all conductor surfaces, except the ports, where currents are fed. There, one assumes a purely normal current flow, i.e.,  $\tilde{E}_0$  has no tangential component and the potential is constant. Its value at each port represents the source and has to be chosen according to the desired field characteristics.

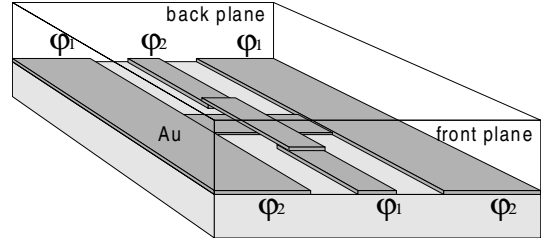


Fig. 1. Magneto-quasi-static analysis of an MMIC airbridge structure: Potential values at the ports, used to determine the static excitation current.

Fig. 1 illustrates this choice of potential distributions at the ports for a coplanar air-bridge, when considering the coplanar mode. Beyond the port metalization surfaces, all other conductor surfaces within the three dimensional structure are terminated by perfect magnetic conductors.

After solving (9) for a given source distribution the magnetic field can be found using (2).

### C. Electrostatic field solution

The electrostatic field solution is restricted to non-conducting regions. It can be found using equations (10) and (11) and replacing  $D_\sigma$  with  $D_\epsilon$ . The structure is surrounded by magnetic and/or electric walls, respectively. For the airbridge configuration in Fig. 1, the front and back plane have to be terminated by magnetic walls. To each of the non-connected parts of the metalization, a different potential value must be assigned.

### D. Modified MGEs and correction factors

In order to incorporate the quasi-static field solutions in the dynamic analysis, one modifies the integral quantities, voltages ( $e, h$ ) currents ( $i$ ), and fluxes ( $d, b$ ), in eqns. (1)...(7). The accuracy of the first-order FD integral approximation is improved by introducing correction factors  $cl$  and  $cf$  for line integrals and surface integrals, respectively. The correction factors are obtained from a high-resolution (quasi-static) field computation as shown in Fig. 2 [4].

From the theoretical point of view, implementing the correction factors can be understood as introducing

artificial anisotropic materials, which replace the original material configuration.

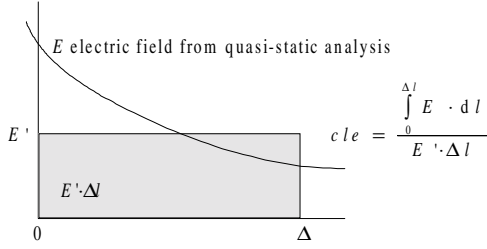


Fig. 2. Accuracy improvement by correction factor (example for electric line integral): The simple form  $E' \cdot \Delta l$  is replaced by  $E' \cdot \Delta l \cdot c l e$  in order to give the same integral value as for the high-resolution analysis.

### III. THE HYBRID PROCEDURE

The hybrid FD method comprises a quasi-static and a dynamic part. The quasi-static field computations are performed on a fine grid, the dynamic analysis on a coarse one.

Regarding the procedure, first the coarse and fine grids are generated. Then, the quasi-static field computations are performed, correction factors are calculated and stored in external files. In the next step, an eigenvalue problem is solved on the coarse grid at the ports of a given structure (e.g., the front and the back plane of the airbridge in Fig. 1), which is necessary to determine the S parameters. The resulting eigenmodes are then used as excitations of the 3D dynamic field computations. Finally, the S parameters are extracted.

### IV. VERIFICATION

In order to verify the new hybrid FD method in frequency domain (hyb. FDFD), the MMIC-typical coplanar structures in Fig. 3, a CPW short-stub and an airbridge, are studied. The conventional FD method (FDFD) serves as a reference [1].

In Figs. 4 – 6, the results of the new hybrid method are compared to conventional FDFD. For the CPW short-stub, the magnitude of the reflection coefficient  $S_{11}$  is plotted in Fig. 4. We find differences of less than 0.12 degree over the entire frequency range.

Further verification of the hybrid method is done comparing the results for two airbridges of different dimensions. In Fig. 5, reflection  $|S_{11}|$  / dB is plotted as a function of frequency. The agreement between the hybrid and the conventional method is good, only at 100 GHz small deviations are observed.

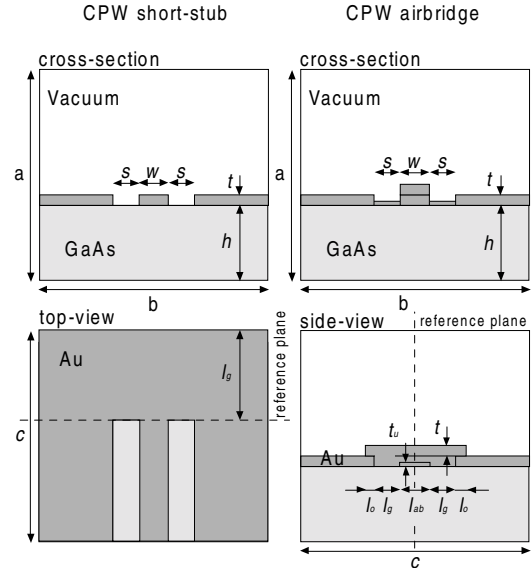


Fig. 3. The two structures under investigation: CPW short-stub and airbridge.

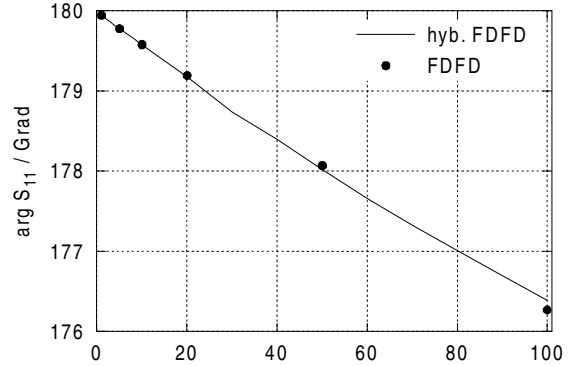


Fig. 4. Reflection coefficient of the CPW short in Fig. 4: magnitude  $S_{11}$  against frequency (dimensions:  $s = 15 \mu\text{m}$ ,  $w = 20 \mu\text{m}$ ,  $t = 3 \mu\text{m}$ ,  $h = 200 \mu\text{m}$ ,  $l_s = 100 \mu\text{m}$ , enclosure:  $a = 703 \mu\text{m}$ ,  $b = 250 \mu\text{m}$ ,  $c = 700 \mu\text{m}$ ; material properties:  $\epsilon_r = 12.9$ ,  $\sigma = 30 \text{ S}/\mu\text{m}$ ).

In practical design, a second parameter is to be considered describing the airbridge, which is its influence on transmission phase, the effective length extension  $\Delta l_{\text{CPW}} = -\arg S_{12} / \beta_{\text{CPW}}$ . Fig. 6 presents the data for airbridge 1 and 2. The negative sign indicates that the electrical length reduces when inserting the airbridge. The differences of the two FD versions are smaller than  $0.3 \mu\text{m}$  for both bridges, which is well below the practical requirements and proves accuracy and usefulness of the hybrid approach.

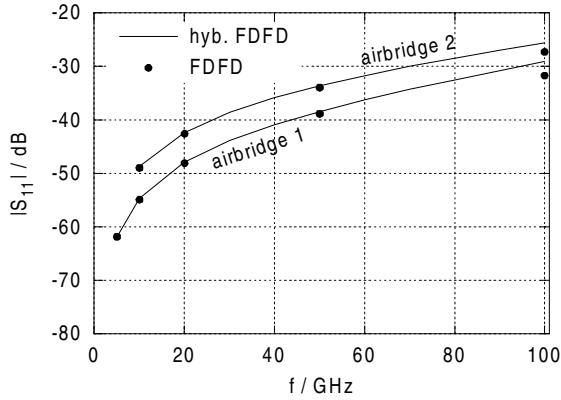


Fig. 5. Reflection magnitude  $|S_{11}|$  / dB of the airbridges according to Fig. 3 against frequency (airbridge 1:  $s = 15 \mu\text{m}$ ,  $w = 20 \mu\text{m}$ ,  $t = 3 \mu\text{m}$ ,  $h = 175 \mu\text{m}$ ,  $t_u = 0.4 \mu\text{m}$ ,  $l_o = 3 \mu\text{m}$ ,  $l_g = 10 \mu\text{m}$ ,  $l_{ab} = 30 \mu\text{m}$ ; enclosure:  $a = 481 \mu\text{m}$ ,  $b = 250 \mu\text{m}$ ,  $c = 672 \mu\text{m}$ ; material properties:  $\epsilon_r = 12.9$ ,  $\sigma = 30 \text{ S}/\mu\text{m}$ ; airbridge 2: dimensions:  $s = 15 \mu\text{m}$ ,  $w = 20 \mu\text{m}$ ,  $t = 3 \mu\text{m}$ ,  $h = 175 \mu\text{m}$ ,  $t_u = 1.5 \mu\text{m}$ ,  $l_o = 5 \mu\text{m}$ ,  $l_g = 10 \mu\text{m}$ ,  $l_{ab} = 20 \mu\text{m}$ ; enclosure:  $a = 681 \mu\text{m}$ ,  $b = 250 \mu\text{m}$ ,  $c = 650 \mu\text{m}$ ; material properties:  $\epsilon_r = 12.9$ ,  $\sigma = 30 \text{ S}/\mu\text{m}$ ).

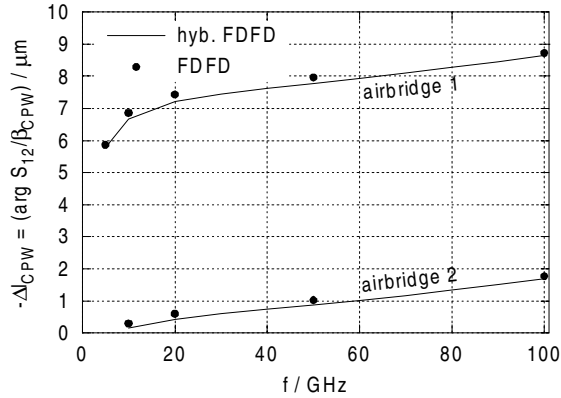


Fig. 6. Effective length extensions  $-\Delta l_{\text{CPW}} = \arg S_{12} / \beta_{\text{CPW}}$  of the CPW airbridges in in Fig. 5 as a function of frequency.

Regarding the computational efforts, the hybrid method requires about 1/6 of the the conventional method for the airbridges, while for the short stub the value is about 1/3. With the new method, one has to run only a single high-resolution magneto-quasi-static field computation per frequency point. In conventional analysis, however, as many field computations as modes at the ports are considered must be performed. Moreover, the better matrix condition of the magneto-quasi-static linear system should allow for further speed-up in analysis. The memory requirements are almost the same so far, since the magnetic quasi-static case involves the same number of unknowns as its dynamic counterpart. This can be improved, however, when applying the correction-factor

approach only to subregions of a structure, preferably those with critical field resolution.

## V. CONCLUSIONS

The incorporation of quasi-static field solutions into the finite-difference method is shown to give a marked improvement in CPU time against the conventional FD method while maintaining accuracy. This holds also in the lossy case. It is of particular interest here, since skin depth increases the required resolution compared to the lossless case. Systematic exploitation of the combined quasi-static and dynamic analysis will allow to study more complex structures and to speed up design process.

## ACKNOWLEDGEMENT

This project is funded by the Deutsche Forschungsgemeinschaft (DFG) under contract He 1676/12.

## REFERENCES

- [1] W. Heinrich, "Full-wave analysis of conductor losses on MMIC transmission lines," *IEEE Trans. Microwave Theory and Tech.*, vol. 38, pp. 1468 – 1472, 1990.
- [2] D. B. Shorthouse and C. J. Railton, "The incorporation of static field solutions into the finite difference time domain algorithm," *IEEE Trans. Microwave Theory and Tech.*, vol. 40, pp. 986 – 994, 1992.
- [3] I. J. Craddock and C. J. Railton, "A new technique for the stable incorporation of static field solutions in the FDTD method for the analysis of thin wires and narrow strips," *IEEE Trans. Microwave Theory and Tech.*, vol. 46, pp. 1091 – 1096, 1998.
- [4] M. Kunze and W. Heinrich, "Efficient FD formulation for lossy waveguide analysis based on quasi-static-field characteristics," *IEEE Microwave and Guided Wave Letters*, vol. 9, pp 499 – 501, 1999.
- [5] M. Kunze and W. Heinrich, "Efficient analytical description of metal loss in finite-difference waveguide analysis," in *2000 European Microwave Conference Proceedings*, Paris, vol. 1, pp. 71 – 74, 2000.
- [6] M. Kunze and W. Heinrich, "Analytical description of metal loss in finite-difference transmission-line analysis," to be published in *IEEE Trans. Microwave Theory and Tech.*
- [7] T. Weiland, "On the unique numerical solution of maxwellian eigenvalue problems in three dimensions," *Particle Accelerators*, vol. 17, pp. 227 – 242, 1985.
- [8] S. Lindenmeier, P. Russer and W. Heinrich, "Applications of the hybrid dynamic-static finite difference approach on 3D-MMIC structures," *13<sup>th</sup> annual review of progress in applied computational electromagnetics*, Monterey, pp. 1182 – 1189, 1997.
- [9] K. Beilenhoff, W. Heinrich and H.L. Hartnagel, "Improved finite-difference formulation in frequency domain for three-dimensional scattering problems", *IEEE Trans. Microwave Theory and Tech.*, vol. 40, pp. 540 – 546, 1992.